

Anti windup GPC speed controller for induction machine based on Youla parametrization

Khelifa Khelifi Otmane¹

In the induction motor indirect vector control system, because of its physical limitations, the large step change in the speed command and/or load would eventually cause the so-called “integral windup phenomenon” which causes unexpected behavior of the system. To counteract this problem, an anti-windup generalized predictive speed control method is proposed by using the Youla parametrization. As first step, the design of an initial GPC controller based on its polynomial equivalent structure is required. Then, thanks to the Youla parametrization, this controller is retuned considering two specifications. The first is a frequency specification on the quadratic component of stator current response to the speed reference. And the second is a time domain constraint on the measured speed response to the speed reference. These constraints are formulated within a convex optimization framework. The simulation results proved the efficiency of the present design method.

Keywords: amplitude saturation, anti windup controller, generalized predictive control, induction motor control, Youla parameterization

1 Introduction

The generalized predictive control (GPC) [1] is an advanced technique of process control. It has been successfully implemented in many industrial applications for last two decades [2], it is due to its robustness, optimality and ability to face uncertainty. Therefore, GPC applications to electrical drives are explored and they involve in largely research laboratories [3–7]. Some authors use the GPC algorithm in cascade form to control several loops of the electrical motor [8, 9], and others adopt the multivariable GPC formulation in order to control several variables of the engine [10].

Even today, the induction motor (IM) stands out as the motor of choice in wide range of applications especially in industrial drives. This, thanks to its higher efficiency, low ripple of torque, lower inertia, high initiate torque, robust architecture and its low cost. In high performance drive system, the field oriented control (FOC) is commonly employed and it is the famous technique used in the induction motor speed control. It is due to its unique characteristics like high efficiency, good power factor and perfectly reliable [11]. The FOC method guarantees the decoupling of torque and flux control commands of the induction motor, so that the induction motor can be controlled linearly like a separate excited DC motor.

Usually, voltage source inverters (VSI) with pulse width modulation (PWM) are used to drive IM. Thus, the overall control system consists typically of an inner current control loop and an outer speed control loop in cascade. The studies that employed GPC laws to control induction motors, provide very satisfactory results in terms of robustness, optimality and ability to face un-

certainty, compared to the classical regulators such as PI/PID controllers [12]. In absence of system constraints, it is possible to obtain the optimal solution in an analytic (explicit) form and hence the GPC control laws are pre-calculated off-line. Therefore, as final step, the GPC controller can be synthesized in its numerical polynomial equivalent structure RST (Reference Signal Tracking) which has a 2DOF (two degree of freedom structure) and comprises of three polynomials namely R, S and T. The RST configuration has become very useful in industrial applications because of their structural simplicity and easy implementation.

In practice, the mentioned electrical drive is a difficult engineering problem, especially in high speed control, since it suffers various restrictions, such as restrictions on power inverter's and maximum allowable current of the motor. If the GPC speed controller is designed in a linear region without regard to any constraint, it can generate an exceeded q-axis current reference for the GPC current controller in dynamic and high speed profiles which leads to an over modulation in the inverter. Also, this current command is practically limited to a prescribed maximum value depended on the magnetic saturation, the inverter maximum current limit and the overheating of stator windings.

Then, the close-loop performance will be significantly deteriorated with respect to the expected linear performance referred as the so-called windup phenomenon, which causes big overshoot on the speed response, slow settling time, and sometimes, even instability in the system. Hence, to safeguard the motor and the power electronics, the control of the IM needs the use of sophisti-

¹ Blida 1 University, Department of Automatic and Electrotechnic, BP 270 Route de Soumaa, Blida, Algeria, khelifi_ot_uhbc@yahoo.fr

cated control that respects these restrictions, while keeping a simple structure designing.

A rational way to handle this problem of windup is to take constraints into account at the stage of control design. However, this a priori design approach has a high computational cost and the resulting control law can be complicated [2, 4].

A more common approach design strategy is a two-step paradigm in which a linear control design satisfying all nominal performance specifications is performed first ignoring the saturation constraints, then an additional compensator to the linear controller is designed to minimize the adverse effects of anti-windup on the closed-loop performance which can take place during saturation [13]. The design based on this second approach is relatively simple design scheme from the viewpoint that the linear performance recovers when the saturation does not occur.

The aim of this paper is to employ an effective and simple design scheme of an anti-windup GPC speed controller based on the Youla parametrization according to the results provided by P. Rodriguez and D. Dumur [14]. The authors in [14] present a unified off-line method based on Youla parametrization to retune an initial GPC law while preserving its two degrees of freedom structure. This parametrization is fulfilled via convex optimization in terms of two free parameters Q_1 and Q_2 in which a separation is made between the closed loop features and the tracking behavior. As a result, the Q_2 can modify only the input-output transfer function without influencing on the closed loop performances. In this paper, we will investigate this feature on an electrical drive to prevent the wind up phenomenon.

2 System modelling

By adopting the traditional assumptions of the vector control of the induction machine, the model in the reference axes d, q related to the rotating field is given in the

form [15]

$$\begin{aligned}
 v_{ds} &= (R_s + \sigma L_s s) i_{ds} - e_{ds}, \\
 v_{qs} &= (R_s + \sigma L_s s) i_{qs} - e_{qs}, \\
 \varphi_r &= \left(\frac{M_m}{1 + T_r s} \right) i_{ds}, \\
 C_{em} &= \frac{p L_m}{L_r} \varphi_r i_{qs}, \\
 \Omega &= \frac{1}{f_r + J s} (C_{em} - C_r),
 \end{aligned}
 \tag{1}$$

where are: s – Laplace operator; v_{ds}, v_{qs} – stator voltages; i_{ds}, i_{qs} – stator currents; φ_r – rotor flux, Ω – rotation speed; C_{em}, C_r – electromagnetic and load torques respectively; J – moment of inertia; L_r, L_s, L_m – rotor, stator and mutual inductances; p – number of pole pairs; f_r – friction coefficient; R_r, R_s – rotor and stator resistance; σ – dispersion coefficient; $T_r = L_r/R_r$ – rotor time constant and the voltage compensation terms are

$$\begin{aligned}
 e_{ds} &= \sigma \omega_s L_s i_{qs}, \\
 e_{qs} &= -\frac{L_m}{L_r} \varphi_r - \sigma \omega_s L_s i_{ds},
 \end{aligned}
 \tag{2}$$

where ω_s is the synchronous speed.

The electrical pole of the induction motor can be neglected because it is faster than the mechanical pole. Considering that the block inverter has neither dynamics nor gain in Fig. 1, it is possible to obtain the following transfer functions corresponding respectively to the electric and mechanics modes

$$\begin{aligned}
 G_i(s) &= \frac{1}{R_s + \sigma L_s s}, \\
 G_s(s) &= \frac{1}{f_r + J s}.
 \end{aligned}
 \tag{3}$$

As the GPC controllers are of discrete type, the transfer functions (3) must be transformed into a discrete time

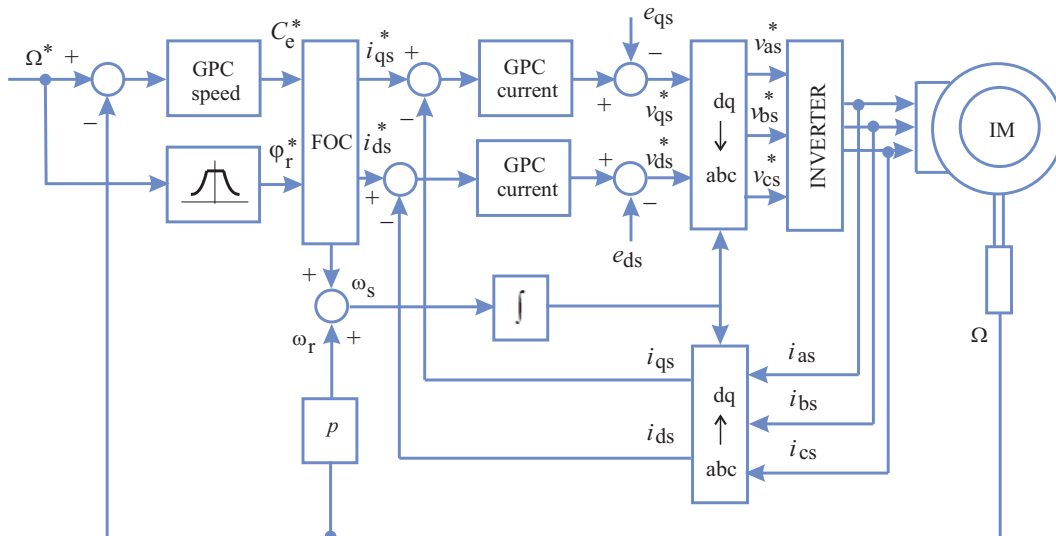


Fig. 1. Block diagram of an induction motor drive based on GPC controllers

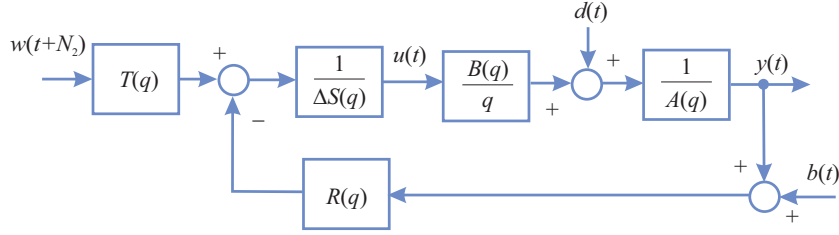


Fig. 2. GPC Equivalent polynomial RST controller

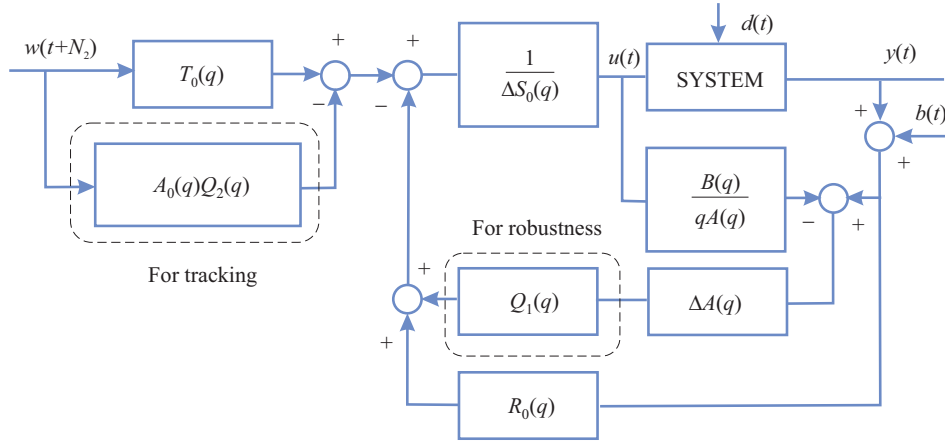


Fig. 3. GPC_RST controller with Youla parametrization

transfer functions. Then, using the ZOH (zero-order hold) discretization method, the z -transform of the process transfer functions (3) can be written as

$$\begin{aligned} G_i(q) &= \frac{A_i(q)}{qB_i}, \\ G_s(q) &= \frac{A_s(q)}{qB_s(q)}. \end{aligned} \quad (4)$$

The transfer functions presented above are the models used in the GPC controllers design for the speed and currents respectively.

Figure 1 shows the block diagram of the induction motor drive based on the FOC scheme. The field weakening assures that the flux reference decreases when the nominal speed of the motor has been exceeded. The $abs \Rightarrow dq$ block get i_{as}, i_{bs} and i_{cs} motor stator currents, using the Park's transformation, while $dq \Rightarrow abs$ block makes the reverse Park's transformation.

$$A(q)y(t) = B(q)u(t) + \frac{\xi(t)}{\Delta(q)}, \quad (5)$$

where $u(t)$ and $y(t)$ are the discrete time ($t = 0, 1, 2 \dots$) plant input and output and A and B are polynomials in backward shift operator q^{-1} derived from (5) and $\Delta(q) = 1 - q^{-1}$, while $\xi(t)$ is an uncorrelated random sequence. The j -step ahead prediction over the costing

horizons $N_1 \leq j \leq N_2$ is given by

$$\begin{aligned} y(t+j) &= \underbrace{F_j(q)y(t) + H_j(q)\Delta u(t-1)}_{\text{free response}} + \underbrace{G_j(q)\Delta u(t+j-1) + J_j(q)\xi(t+j)}_{\text{forced response}}, \end{aligned} \quad (6)$$

$F_j(q), G_j(q), H_j(q)$ are polynomials obtained by solving Diophantine equations.

To achieve optimal command values, the GPC uses a quadratic cost function defined as

$$J(N_1, N_2) = \sum_{j=N_1}^{N_2} [\hat{y}(t+j) - w(t+j)]^2 + \lambda \sum_{j=1}^{N_u} [u(t+j-1)]^2, \quad (7)$$

where N_1 and N_2 define the output prediction horizons, and N_u is the control horizon. Here λ is the control weighting factor, w is the reference value, and \hat{y} is the predicted output value. The receding horizon principle assumes that only the first value of the optimal control sequence resulting from the minimization of (5) is applied, so that at the next sampling period the same procedure is repeated. This control strategy leads to a 2-DOF RST, Fig. 2, controller implemented through a difference equation

$$S(q)\Delta(q)u(t) = -R(q)y(t) + T(q)w(t). \quad (8)$$

So, three GPC-RST controllers will be synthesized, one for the outer speed control loop denoted (GPC speed) and a pair for the inner current loops denoted (GPC current).

Assuming the design of the initial GPC speed controller has been performed with R_0, S_0, T_0 , and N_1, N_2, N_u, λ , adjusted to satisfy certain closed loop performance. We notice in Fig. 1, that the GPC speed controller does not have output magnitude limiter, and therefore, the reference of the electromagnetic torque C_{em}^* , subsequently the current command i_{qs}^* can take values relatively large in transient regimes, especially, in high speed profiles, and, as a consequence, the system drive can be damaged by the large control action. The main goal of this work is to avoid the over values of the currents without incorporating a limiter at the output and without losing the close loop performance obtained by the initial GPC speed controller. It will be carried out by retuning the initial controller based on Youla parametrization. The resulting controller must respect the prescribed limits.

3 Retuned GPC speed using Youla parameterization

According to the work presented in [1], the Youla parameterization of the initial GPC speed controller (R_0, S_0, T_0) leads to the following stabilizing polynomials

$$\begin{aligned} T(q) &= T_0(q) - A_o(q)Q_2(q), \\ R(q) &= R_0(q) + \Delta A(q)Q_1(q), \\ S(q) &= S_0(q) - qB(q)Q_1(q), \end{aligned} \quad (9)$$

where Q_1 and Q_2 are stable transfer functions. The corresponding block diagram is shown in Fig. 3.

From the diagram in Fig. 3, we can conclude that the parameter Q_1 modifies the closed loop features keeping the input output transfer unchanged, whereas, the parameter Q_2 modifies only the input-output transfer function. In the following we set Q_l to zero since the closed loop performance is fulfilled by the initial controller design, then Q_2 will be used to retune this initial controller modifying the input-output behavior in order to prevent the undesired high control signal at the output of the GPC speed controller.

Q_2 is designed to satisfy two kinds of specifications – frequency and time specifications. Where the signals w, y , and u correspond receptively to the speed reference Ω^* , measured speed Ω , and the current command i_{qs}^* .

Let H_{yw} be the transfer function between the input w and the output y

$$H_{yw} = \frac{B}{qA_oA_c}(T_0 - A_oQ_2), \quad (10)$$

where $A_oA_c = \Delta AS_0 + BR_0/q$ is the characteristic polynomial of the closed loop obtained with the initial controller $R_0S_0T_0$ which is split into a control polynomial A_c and an observer polynomial A_o .

In the steady state, the output y must equal the reference w . To ensure that, the following relation must be valid

$$\frac{y}{w} = \frac{B}{qA_oA_c}(T_0 - A_oQ_2) \Big|_{q=1} = 1. \quad (11)$$

It is thus necessary that $Q_2 = 0$ for $q = 1$. This can be obtained simply by forcing in Q_2 a term $\Delta = 1 - q^{-1}$ in the numerator

$$Q_2 = \Delta Q'_2. \quad (12)$$

3.1 Frequency specifications

We consider a frequency specification on the control signal response to the input. Let H_{uw} be the transfer function between the input w and the control signal u

$$H_{uw} = \frac{u}{w} = \frac{A}{A_oA_c}(T_0 - A_o\Delta Q'_2). \quad (13)$$

This, being linearly parameterized by the Youla parameter Q_2 , means the frequency specifications are convex in Q_2 . The minimization of the transitory command is achieved by minimizing an H_∞ norm of the transfer function H_{uw} weighted by a transfer function W .

$$\min_{Q'_2 \in \mathcal{RH}_\infty} \|H_{uw}W\|_\infty = \min_{Q'_2 \in \mathcal{RH}_\infty} \left\| \frac{A}{A_oA_c}(T_0 - A_o\Delta Q'_2)W \right\|, \quad (14)$$

where \mathcal{RH}_∞ is the space of all proper and stable transfer functions. The H_∞ norm minimization and the time constraints can be approximated by a minimization under linear inequality constraints, so (14) we can write

$$\begin{aligned} \min_{Q'_2 \in \mathcal{RH}_\infty} \|T_1 + T_2Q'_2\|_\infty = \\ \min_{Q'_2 \in \mathcal{RH}_\infty} \max_{0 < \omega < \pi} \|T_1(e^{-j\omega}) + T_2(e^{-j\omega})Q'_2(e^{-j\omega})\|. \end{aligned} \quad (15)$$

Taking the following polynomial

$$Q'_2 = \sum_{i=0}^{n_q} \alpha_i Q'_{2i}, \quad (16)$$

and replacing half of the unit disk by a finite grid, the last relation becomes

$$\begin{aligned} \left\| \underbrace{T_1(e^{-j\theta_k}) \mathbf{I}}_{\mathbf{T}_{1k}} + \underbrace{T_2(e^{-j\theta_k}) [Q'_{20}(e^{-j\theta_k}), \dots, Q'_{2n_q}(e^{-j\theta_k})]}_{\mathbf{T}_{2k}} \right\| \times \\ \times \left\| \underbrace{\begin{bmatrix} \alpha_0 \\ \dots \\ \alpha_{n_q} \end{bmatrix}}_{\alpha} \right\| \leq \gamma, \end{aligned} \quad (17)$$

with γ being the upper bound of the left-hand side of (15), $\theta_k = \pi(k-1)/(N-1)$ for $k = 1, \dots, N$, and \mathbf{I} is an identity matrix. Finally we get a form

$$\|\mathbf{T}_{1k} + \mathbf{T}_{2k}\| \leq \gamma \quad \text{for } k = 1, 2, \dots, N. \quad (18)$$

This matrix inequality under the form $\|\mathbf{x}\| \leq \gamma$, is approximated by a set of four linear inequalities

$$\begin{aligned} \operatorname{Re}(x) + \operatorname{Im}(x) &\leq \gamma, \\ \operatorname{Re}(x) - \operatorname{Im}(x) &\leq \gamma, \\ -\operatorname{Re}(x) + \operatorname{Im}(x) &\leq \gamma, \\ -\operatorname{Re}(x) - \operatorname{Im}(x) &\leq \gamma. \end{aligned} \quad (19)$$

These inequalities lead to the cost minimization under inequality constraints. Hence, the minimization of the H_∞ norm of the transfer function H_{uw} can be written as

$$\min_{\mathbf{A}\mathbf{X}-\mathbf{B}\leq 0} \mathbf{C}\mathbf{X} \quad (20)$$

with

$$\begin{aligned} \mathbf{A} &= \begin{bmatrix} -1 & \operatorname{Re}(T_{21}) & + & \operatorname{Im}(T_{21}) \\ \vdots & & & \\ -1 & -\operatorname{Re}(T_{2N}) & - & \operatorname{Im}(T_{2N}) \\ -1 & 0 & \dots & 0 \end{bmatrix}_{(4N+1) \times (n_q+2)}, \\ \mathbf{B} &= \begin{bmatrix} -\operatorname{Re}T_{11} & -\operatorname{Im}T_{11} \\ \vdots & \\ -\operatorname{Re}T_{1N} & -\operatorname{Im}T_{1N} \\ 0 & \end{bmatrix}_{4(N+1) \times 1}, \quad \mathbf{X} = \begin{bmatrix} \gamma \\ a_0 \\ \vdots \\ a_{n_q} \end{bmatrix}_{(n_q+2) \times 1}, \\ \mathbf{C} &= [1 \quad 0 \quad \dots \quad 0]_{1 \times (n_q+2)}. \end{aligned}$$

3.2 Time specifications

In this stage a time specification on the output signal to the input is considered. The transfer function becomes

$$H_{yw} = \frac{y}{w} = \frac{B}{qA_0A_c}(T_0 - A_0\Delta)Q'_2. \quad (21)$$

The Youla parameterization allows linear dependency between the transfer function H_{yw} and the Youla parameter Q_2 as shown by (21). So, the time specifications are also convex in Q_2 .

Similarly, as in frequency specifications case,(21) can be written as

$$H_{yw} = \tilde{T}_1 + \tilde{T}_2 Q'_2. \quad (22)$$

Also we can write

$$(y(t))/w(t) = \tilde{T}_1 + \tilde{T}_2 \sum_{i=0}^{n_q} \alpha_i Q'_{2i}. \quad (23)$$

Then, the output $y(t)$ is

$$y(t) = (\tilde{T}_1 + \tilde{T}_2(\alpha_0 Q'_0 + \dots + \alpha_{n_q} Q'_{n_q}))w(t). \quad (24)$$

We note

$$y_1(t) = \tilde{T}_1 w(t) \quad \text{and} \quad y_2(t) = \tilde{T}_2 Q'_i w(t)$$

to become

$$y(t) = y_1(t) + [y_{20}(t) \ y_{21}(t) \ \dots \ y_{2n_q}(t)] \begin{bmatrix} \alpha_0 \\ \vdots \\ \alpha_{n_q} \end{bmatrix}. \quad (25)$$

Then

$$\begin{aligned} y(t) - y_{\max}(t) &\leq 0 \\ -y(t) + y_{\min}(t) &\leq 0 \end{aligned} \quad \text{for } t = t_0, t_1, \dots, t_{N_t}. \quad (26)$$

Finally, we obtain the linear inequalities constraints correspond to the time specifications as

$$\tilde{\mathbf{A}}\mathbf{X} - \tilde{\mathbf{B}} \leq 0 \quad (27)$$

where

$$\begin{aligned} \tilde{\mathbf{A}} &= \begin{bmatrix} y_{20}(t_0) & y_{21}(t_0) & \dots & y_{2n_q}(t_0) & 0 \\ y_{20}(t_1) & y_{21}(t_1) & \dots & y_{2n_q}(t_1) & 0 \\ \dots & \dots & \dots & \dots & \dots \\ y_{20}(t_{N_t}) & y_{21}(t_{N_t}) & \dots & y_{2n_q}(t_{N_t}) & 0 \\ -y_{20}(t_0) & -y_{21}(t_0) & \dots & -y_{2n_q}(t_0) & 0 \\ -y_{20}(t_1) & -y_{21}(t_1) & \dots & -y_{2n_q}(t_1) & 0 \\ \dots & \dots & \dots & \dots & \dots \\ -y_{20}(t_{N_t}) & -y_{21}(t_{N_t}) & \dots & -y_{2n_q}(t_{N_t}) & 0 \end{bmatrix}_{(2N_t+2) \times (n_q+2)} \\ \tilde{\mathbf{B}} &= \begin{bmatrix} y_{\max}(t_0) - y_1(t_0) \\ \vdots \\ y_{\max}(t_{N_t}) - y_1(t_{N_t}) \\ -y_{\min}(t_0) + y_1(t_0) \\ \vdots \\ -y_{\min}(t_{N_t}) + y_1(t_{N_t}) \end{bmatrix}_{(2N_t+2) \times 1} \end{aligned}$$

by adding these new constraints (27) to the optimization problem defined by (20), we obtain the following global optimization problem which can be solved with a classical algorithms

$$\min \begin{pmatrix} \mathbf{A} \\ \tilde{\mathbf{A}} \end{pmatrix} \mathbf{x} - \begin{pmatrix} \mathbf{B} \\ \tilde{\mathbf{B}} \end{pmatrix} \leq 0 \quad \mathbf{C}\mathbf{X}. \quad (28)$$

4 Simulation tests

In the next, the retuned GPC controller previously developed has been applied on the induction motor drive. The motor is a squirrel-cage type induction machine of 1.1 kW and 1500 rpm, where its parameters are shown in the appendix.

As a first step, three initial GPC controllers have been designed, one for the outer speed control loop (GPC speed) and two for the inner current loops (GPC current) Fig. 1. The inner system is sampled at $T_i = 0.05$ ms, and the outer system is sampled at $T_s = 1$ ms. According to the rules given in [16],

$$\begin{aligned} N_1 &= \frac{\text{process dead time}}{\text{sample period}}, \\ N_2 &= \frac{\text{process rise time}}{\text{sample period}}, \end{aligned}$$

N_u = number of poles near the stability boundary.

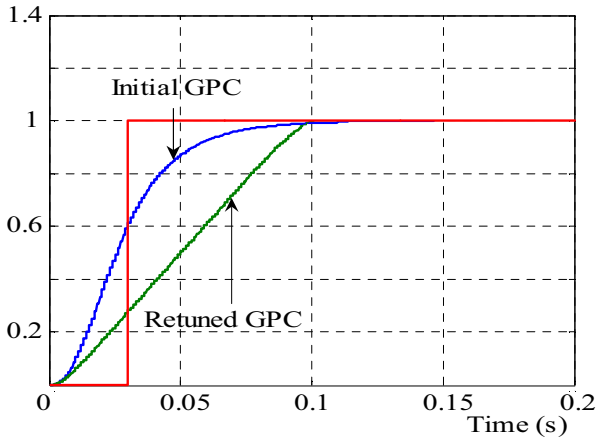


Fig. 4. Step response and time domain template

The following GPC parameters for both controllers were selected

$$\begin{aligned}
 N_1 = 1, N_2 = 30, N_u = 1 & \text{ for the speed loop,} \\
 N_1 = 1, N_2 = 5, N_u = 1 & \text{ for the current loop.}
 \end{aligned}$$

Using the simplified model (4), the simulation shows that the controller GPCs provides a fast tracking behavior but the control action is very high (reaches about 400% for the nominal value), which is unacceptable in electrical drives. This inconvenient justifies the design of the modified controller that will reduce the control action

in the transitory regime. For that purpose, minimization problem (16) must be solved considering, as time specifications, a time domain template for which the system preserves the time response obtained with the initial controller. We chose $N_t = 200$ the number of points of the time response taken into account by the template *ie* horizon of 0.2s). The chosen weighting function W is

$$W = \frac{1 - 0.8q}{0.2} \tag{29}$$

The research of the Q_2 parameter has been achieved with 100-order polynomial and with 180 points for the transfer norm calculation. The obtained polynomial is then approached by a transfer function [17].

Figure 4 illustrates the step response of the simplified model connected to both the initial and modified controller and it also shows the template which must be respected.

The time response to a step input and to the perturbation at 0.2s is shown in Fig. 5. Figure 6 depicts the control signal where the results obtained with the initial controller are superimposed in comparison. We note that the dynamic of the disturbance rejection remains unchanged. In addition, the transitory command is reduced and the dynamics of the input/output behavior respects the imposed template.

Now, let us examine this procedure on the complete drive system shown in Fig. 1 under different conditions

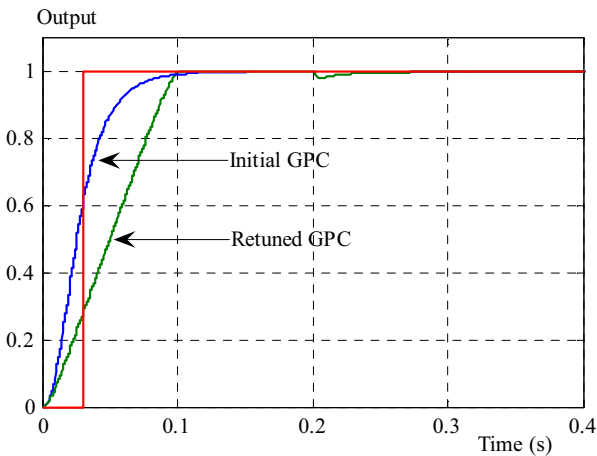


Fig. 5. Temporal response of the system connected to the initial and retuned GPC

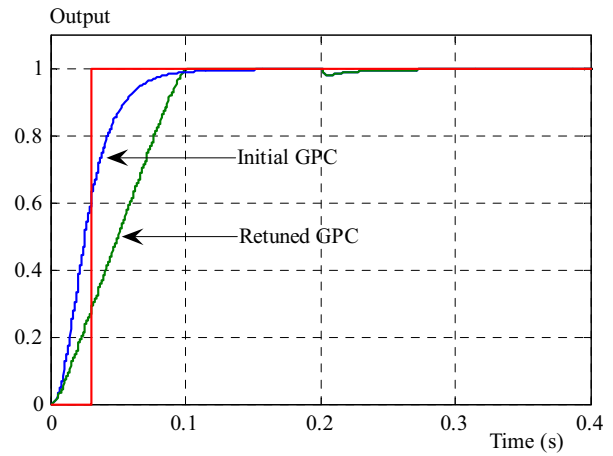


Fig. 6. Control signal of the system connected to the initial and retuned GPC

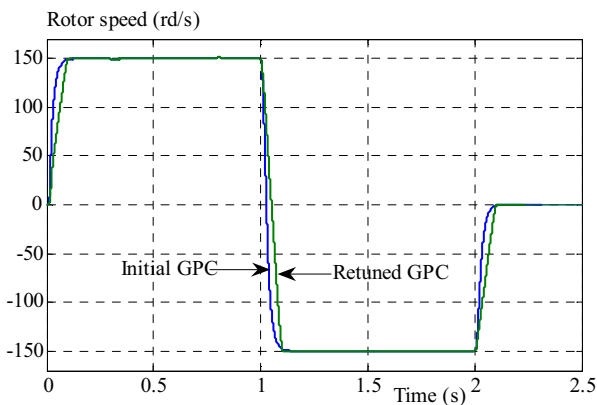


Fig. 7. Rotor speed of the induction motor drive

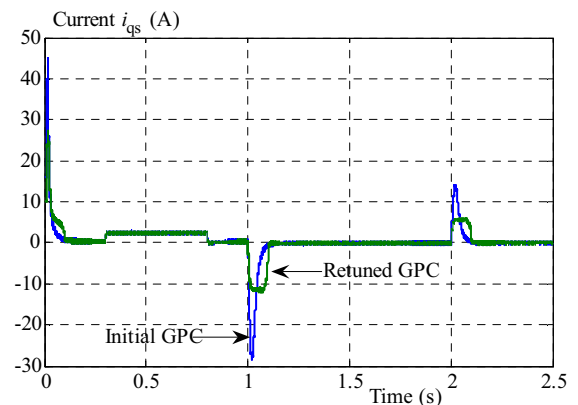


Fig. 8. Quadratic component of stator current i_{qs}

such as motor speed and load torque variations. The drive system nameplate data and parameters are shown in the Appendix. A rectangular form of motor speed reference is chosen. At first, the motor initially operates under unload conditions with a speed rotor equals 150 rd/s. Between $t = 0.3$ s and $t = 0.8$ s, the load torque is stepped to 5 Nm in order to examine the impact of the load condition. The speed is reversed from 150 rd/s at 1 s to -150 rd/s at 2 s. After that, the motor is stopped.

Figure 7 and 8 depicts, respectively, the rotor speed and the quadratic component of the stator current that represents the control signal. It is easier to see that the quadratic component of the stator current is minimized in the transient regime thanks to the retuned GPC regulator, while this controller preserves the same time response of the system and the same dynamic of the disturbance rejection obtained by the initial GPC controller.

These results demonstrate that the proposed method is efficient compared the conventional methods with anti-windup scheme that use a limiter in the output of the controller.

5 Conclusions

This paper has stated the effect of the caused by the high transitory current control of an induction motor generated by a GPC speed controller caused by the fast and large step change in the speed reference. For that, three generalized predictive controllers are used to drive the machine, two inner ones to control the currents and an outer one to control the speed. Then, by means of the Youla parameterization, the outer controller has been retuned such that frequency and time-domain constraints are satisfied can be formulated as a convex linear optimization problem. The resulting controller has two advantages. Firstly, it can minimize the current command in the transitory regime, and secondly, it keeps the time response of the system obtained before the modification without changing the closed loop behavior. These results are validated by simulations.

Appendix

Motor parameters: 1.1 kW, 1500 rpm, 3.5 A, 220/380 V, 1.14 Wb, 7 Nm, $R_s = 8.1 \Omega$, $R_r = 3.2 \Omega$, $L_s = L_r = 0.48$ H, $L_m = 0.46$ H $J = 0.006$ kg · m².

REFERENCES

[1] D. W. Clarke, C. Mohtadiet, and P. S. Tuffs, "Generalized predictive control -Part I. and II", *Automatica*, vol. 23, no. 2, pp. 137-160, 1987.

[2] E. F. Camacho and C. Bordons, , *Model Predictive Control*, Springer, 2003.

[3] L. Zhang, R. Norman, and W. Shepherd, "Long-Range Predictive Control of current regulated PWM for induction motor drives using the synchronous reference frame", *IEEE Trans. Control Syst. Technol.*, vol. 5, no. 1, pp. 119-126, 1997.

[4] R. Kennel, A. Linder, and M. Linke, "Generalized predictive control (GPC) - ready for use in drive applications?", *Proc. of the IEEE Power Electronics Specialists Conference PESC 01*, pp. 1839-1844, 2001.

[5] A. Linder and R. Kennel, "Model predictive control for electrical drives", *Proc. of the IEEE Power Electronics Specialists Conference PESC 05*, pp. 1793-1799, 2005.

[6] M. Tonnes and H. Rasmussen, "Robust self-tuning control of AC-servo drive", *Proceedings of the European Conference on Power Electronics and Application*, pp. 3049-3053, November , 1991.

[7] D. G. V. d. Fonseca and A. F. A. Dantas, "Explicit GPC Control Applied to an Approximated Linearized Crane System", *Journal of Control Science and Engineering*, vol. , 2019.

[8] R. Kennel, A. Linder, and M. Linke, "Generalized Predictive Control (GPC)-ready for use in drive applications?", *Proceedings of the IEEE 32nd Annual Power Electronics Specialists Conference*, pp. 1839-1844, Vancouver, Canada, June , 2001.

[9] K. Barra and K. Benmahammed, "New extended cascaded predictive control with multiple reference models ECGPC/MRM of an induction motor drive with efficiency optimization", *Journal of Electrical Engineering*, vol. 58, no. 2, pp. 71-78, 2007.

[10] E. S. d. Santana, E. Bim, and W. C. d. Amaral, "A predictive algorithm for controlling speed and rotor flux of induction motor", *IEEE Transactions on Industrial Electronics*, vol. 55, no. 12, pp. 4398-4407, 2008.

[11] B. K. Bose, "Modern Power electronics and AC drives", *The University of Tennessee, Knoxville, USA, Prentice Hall*, A Treatise on Electricity and Magnetism, 3rd ed, vol. 2, Oxford: Clarendon, 2002.

[12] W. A. Silva and A. B. S. Junior, "Generalized predictive control robust for position control of induction motor using field-oriented control", *Electrical Engineering*, vol. 97, pp. 195-204, 2015.

[13] M. V. Kothare, P. J. Campo, M. Morari, and C. N. Nett, "A unified framework for the study of anti-windup designs", *Automatica*, vol. 30, no. 12, pp. 1869-1883, 1994.

[14] P. A. D. D. Rodriguez, "Generalized predictive control robustification under frequency and time-domain constraints", *IEEE Transactions on Control Systems Technology*, pp. 13, pp. 577-587, 2005.

[15] M. Maaziz, P. Boucher, and D. Dumur, "Flux and speed tracking of an induction motor based on nonlinear predictive control and feedback linearization", *IEEE ACC conf. San Diego, USA*, June, 1999.

[16] P. Boucher and D. Dumur, "La commande prdictive", *Collection Mthodes et pratiques de lingnieur*, Editions Technip, Paris, 1996.

[17] J. G. Proakis and D. G. Manolakis, *Digital Signal Processing: Principles, Algorithms and applications*, Englewood Cliffs, NJ: pp. Prentice-Hall, pp. 7196-724, 1996.

Received 10 August 2021